Article

Cite This: *Biomacromolecules* 2018, 19, 3874−3882

pubs.acs.org/Biomac

# Fabrication of Acidic pH-Cleavable Polymer for Anticancer Drug Delivery Using a Dual Functional Monomer

Luping Zheng,[†,‡] Xiaolong Zhang,[†,‡] Yunfei Wang,[†] Fangjun Liu,[†] Jinlei Peng,[†] Xuezhi Zhao,[†] Huiru Yang,[†] Liwei Ma,[†] Baoyan Wang,[†] Cong Chang,*[,§] and Hua Wei*[,†]

[†]State Key Laboratory of Applied Organic Chemistry, Key Laboratory of Nonferrous Metal Chemistry and Resources Utilization of Gansu Province, and College of Chemistry and Chemical Engineering, Lanzhou University, Lanzhou, Gansu 730000, China

[§]Department of Pharmaceutics, School of Pharmacy, Hubei University of Chinese Medicine, Wuhan, Hubei 430065, China

Supporting Information



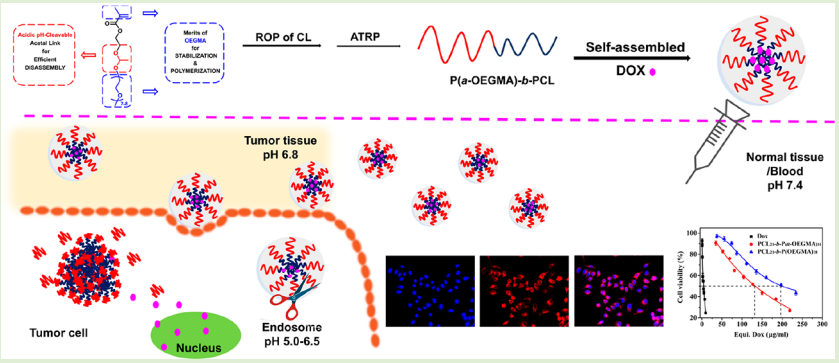


**ABSTRACT:** The preparation of tumor acidic pH-cleavable polymers generally requires tedious postpolymerization modifications, leading to batch-to-batch variation and scale-up complexity. To develop a facile and universal strategy, we reported in this study design and successful synthesis of a dual functional monomer, *a*-OEGMA that bridges a methacrylate structure and oligo(ethylene glycol) (OEG) units via an acidic pH-cleavable acetal link. Therefore, *a*-OEGMA integrates (i) the merits of commercially available oligo(ethylene glycol) monomethyl ether methacrylate (OEGMA) monomer, i.e., hydrophilicity for extracellular stabilization of particulates and a polymerizable methacrylate for adopting controlled living radical polymerization (CLRP), and (ii) an acidic pH-cleavable acetal link for efficiently intracellular destabilization of polymeric carriers. To demonstrate the advantages of *a*-OEGMA ($M_n$ = 500 g/mol) relative to the commercially available OEGMA ($M_n$ = 300 g/mol) for drug delivery applications, we prepared both acidic pH-cleavable poly($\varepsilon$-caprolactone)$_{21}$-*b*-poly(*a*-OEGMA)$_{11}$ (PCL$_{21}$-*b*-P(*a*-OEGMA)$_{11}$) and pH-insensitive analogues of PCL$_{21}$-*b*-P(OEGMA)$_{18}$ with an almost identical molecular weight (MW) of approximately 5.0 kDa for the hydrophilic blocks by a combination of ring-opening polymerization (ROP) of $\varepsilon$-CL and subsequent atom transfer radical polymerization (ATRP) of *a*-OEGMA or OEGMA. The pH-responsive micelles self-assembled from PCL$_{21}$-*b*-P(*a*-OEGMA)$_{11}$ showed sufficient salt stability, but efficient acidic pH-triggered aggregation that was confirmed by the DLS and TEM measurements as well as further characterizations of the products after degradation. In vitro drug release study revealed significantly promoted drug release at pH 5.0 relative to the release profile recorded at pH 7.4 due to the loss of colloidal stability and formation of micelle aggregates. The delivery efficacy evaluated by flow cytometry analyses and an in vitro cytotoxicity study in A549 cells further corroborated greater cellular uptake and cytotoxicity of Dox-loaded pH-sensitive micelles of PCL$_{21}$-*b*-P(*a*-OEGMA)$_{11}$ relative to the pH-insensitive analogues of PCL$_{21}$-*b*-P(OEGMA)$_{18}$. This study therefore presents a facile and robust means toward tumor acidic pH-responsive polymers as well as provides one solution to the trade-off between extracellular stability and intracellular high therapeutic efficacy of drug delivery systems using a novel monomer of *a*-OEGMA with dual functionalities.

## INTRODUCTION

In the past several decades, stimuli-responsive polymers capable of responding to various biorelevant triggers including pH, temperature, and redox potential for structural change or dissociation toward enhanced intracellular therapeutic efficacy have drawn great attention.[1−10] More recently, the development of light-sensitive polymers[11−13] and nanodiamond (ND)@polymer hybrid systems[14−17] have emerged as innovative platforms toward improved efficacy and safety of cancer nanomedicine applications.

Due to the notable pH gradients between the normal and tumor tissues as well as in different cellular compartments, that

Received: June 26, 2018
Revised: August 10, 2018
Published: August 14, 2018




DOI: 10.1021/acs.biomac.8b01001
*Biomacromolecules* 2018, 19, 3874−3882

is, pH 5.5−6.0 for endosomes and pH 4.5−5.0 for lysosomes, while the extracellular pH of tumor microenvironment is pH 6.8, which is slightly lower than the physiological pH 7.4,[18−20] various pH-sensitive polymeric carriers containing acidic pH-cleavable links, such as acetal,[21−23] hydrazone,[24−26] orthoester,[27,28] and carbamate[29] have been successfully designed and synthesized to realize efficiently intracellular deformation of carriers and subsequently promoted release of loaded cargoes.

Although tremendous progress has been made in this field of research, the preparation of tumor acidic pH-cleavable polymers generally requires tedious postpolymerization modifications, leading to batch-to-batch variation and scale-up complexity.[30,31] Specifically, it remains a synthetic challenge to develop polymers containing multiple acid-cleavable links with readily and precisely modulated polymer composition and functionalities. For this purpose, we reported in this study a facile and universal strategy by designing and successfully synthesizing a dual functional monomer, *a*-OEGMA that bridges a methacrylate structure and oligo(ethylene glycol) (OEG) units via an acidic pH-cleavable acetal link (Scheme 1).

**Scheme 1. Schematic Illustration of Structure and Merits of *a*-OEGMA Monomer Developed in This Study**

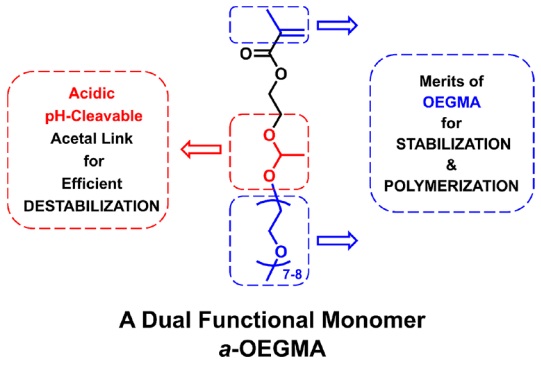


Therefore, the dual functions of *a*-OEGMA lie in (i) the merits of commercially available oligo(ethylene glycol) monomethyl ether methacrylate (OEGMA) monomer, that is, hydrophilicity for extracellular stabilization of particulates and a polymerizable methacrylate for adopting controlled living radical polymerization (CLRP), and (ii) an acidic pH-cleavable acetal link[30,31] for efficiently intracellular destabilization of polymeric carriers.

To demonstrate the advantages of *a*-OEGMA ($M_n$ = 500 g/mol) relative to the commercially available OEGMA ($M_n$ = 300 g/mol) for drug delivery applications, we prepared both acidic pH-cleavable poly($\varepsilon$-caprolactone)$_{21}$-*b*-poly(*a*-OEGMA)$_{11}$ (PCL$_{21}$-*b*-P(*a*-OEGMA)$_{11}$) and pH-insensitive analogues of PCL$_{21}$-*b*-P(OEGMA)$_{18}$ with an almost identical molecular weight (MW) of approximately 5.0 kDa for the hydrophilic blocks, which was shown in our previous study[32] to provide sufficient stability for the self-assembled micelles, by a combination of ring-opening polymerization (ROP) of $\varepsilon$-CL and subsequent atom transfer radical polymerization (ATRP) of *a*-OEGMA or OEGMA. The delivery efficacy of acidic pH-cleavable micelles was evaluated by an in vitro drug release study, confocal microscopy measurements, flow cytometry analyses as well as an in vitro cytotoxicity study, and compared with the pH-insensitive analogues.

## EXPERIMENTAL SECTION

Materials, polymer synthesis and characterizations, in vitro drug loading and drug release study, and in vitro biological assays are provided in the Supporting Information (SI).

**Synthesis of 2-(Vinyloxy)ethyl Methacrylate (VEMA).** VEMA was prepared from 2-(vinyloxy)ethanol and methacryloyl chloride in the presence of triethylamine (TEA).[33] Briefly, 2-(vinyloxy)ethanol (6.281 mL, 70 mmol), TEA (9.730 mL, 70 mmol), was dissolved in 100 mL of anhydrous dichloromethane (DCM). A solution of methacryloyl chloride (6.159 mL, 63.64 mmol) in anhydrous DCM was added dropwise to the above mixture at 0 °C under $N_2$ flow with stirring for a period of 30 min. Then the reaction mixture was further stirred at room temperature for 4 h. After reaction, a white byproduct TEA·HCl was filtrated out. The crude product was concentrated and purified by column chromatography with eluents of ethyl acetate/hexane (1/30, v/v) to obtain 8.30 g of colorless liquid (yield, 84%). $^1$H NMR (400 MHz, $CDCl_3$, ppm, Figure S1): $\delta$ 6.51 (dd, $J$ = 14.4, 6.8 Hz, 1H), 6.15 (s, 1H), 5.59 (s, 1H), 4.40−4.37 (m, 2H), 4.24 (dd, $J$ = 14.0, 2.0 Hz, 1H), 4.06 (dd, $J$ = 6.8, 2.4 Hz, 1H), 3.95−3.93 (m, 2H), 1.95 (s, 3H).

**Synthesis of *a*-OEGMA (Scheme 2).** *a*-OEGMA was prepared from VEMA and methoxypolyethylene glycols (mPEG, $M_n$ = 350 g/mol and 7∼8 pendant EO units) in the presence of a small catalytic amount of *p*-toluenesulfonic acid (PTS) according to the reported procedures.[34] Briefly, VEMA (4.685 g, 30 mmol), mPEG (10.50 g, 30 mmol), and PTS (114.13 mg, 0.6 mmol) was dissolved in 60 mL of anhydrous DCM at room temperature under $N_2$ flow with stirring for a period of 30 min. The reaction mixture was later stirred at 35 °C for 3 days. After reaction, the reaction mixture was concentrated, and further purified by column chromatography with eluents of ethyl acetate/hexane (1/2, v/v) to obtain 11.08 g of colorless liquid (yield, 73%).

**Scheme 2. Synthesis of a Dual Functional Monomer, *a*-OEGMA**

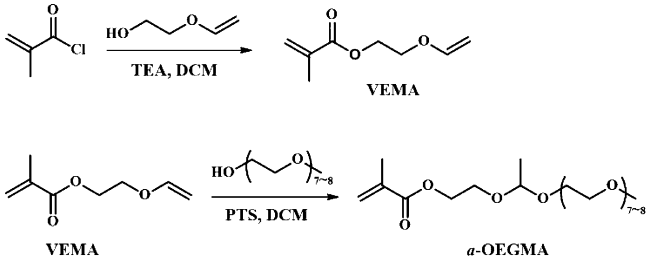


## RESULTS AND DISCUSSION

**Synthesis of PCL-*b*-P(*a*-OEGMA).** The vinyloxy group of VEMA, which acts as an "anchor" site, could be functionalized by alcohols,[35] polyols,[36] and triazoles[37] to generate various functional methacryloyloxy acetals as promising monomers, comonomers, cross-linking agents, building blocks, and starting materials for the synthesis of biologically active substances, therefore, VEMA was used as a precursor for *a*-OEGMA monomer in this study.

Successful synthesis of *a*-OEGMA monomer is confirmed by $^1$H NMR analysis (Figure 1), which reveals the presence of all the characteristic signals of each proton including peaks a and b at 6.12 and 5.57 ppm attributed to the vinyl protons of VEMA, peak d at 3.35 ppm assigned to PEG units, and peaks c and f at 4.84−4.79, and 1.34−1.31 ppm attributable to the protons of acetal methine and adjacent methyl. More importantly, the ratio of the integrated intensity of peaks g to f was calculated to be 2/3, strongly supporting equivalent coupling of VEMA and mPEG. Further characterizations of *a*-



DOI: 10.1021/acs.biomac.8b01001
Biomacromolecules 2018, 19, 3874−3882

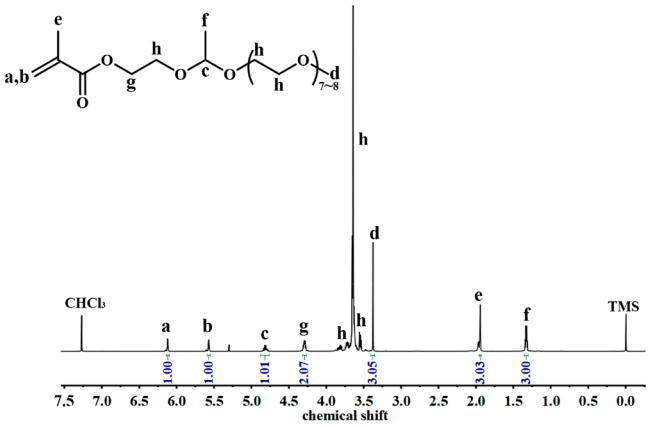


**Figure 1.** $^{1}$H NMR spectrum of *a*-OEGMA in $CDCl_3$.

OEGMA also confirm its successful synthesis including the appearance of a characteristic signal at 99.8 ppm attributed to the acetal link in $^{13}$C NMR spectrum (Figure S2), the presence of all the characteristic absorbance bands in the FT-IR spectrum (Figure S3), and the distribution of molecular ion peaks recorded in the high resolution mass spectrum (HRMS; Figure S4).

To investigate the utility of this new monomer for polymer construction, *a*-OEGMA was next used to prepare target acidic pH-cleavable amphiphilic diblock copolymer, PCL-*b*-P(*a*-OEGMA) by ATRP using ROP-generated PCL-iBuBr as a macroinitiator (Scheme 3). The degree of polymerization (DP) of PCL was first determined to be 21 by $^{1}$H NMR analysis (Figure S5).

**Scheme 3. Synthesis of Acidic pH-Cleavable Diblock Copolymer, PCL-*b*-P(*a*-OEGMA) by Integrated ROP and ATRP**

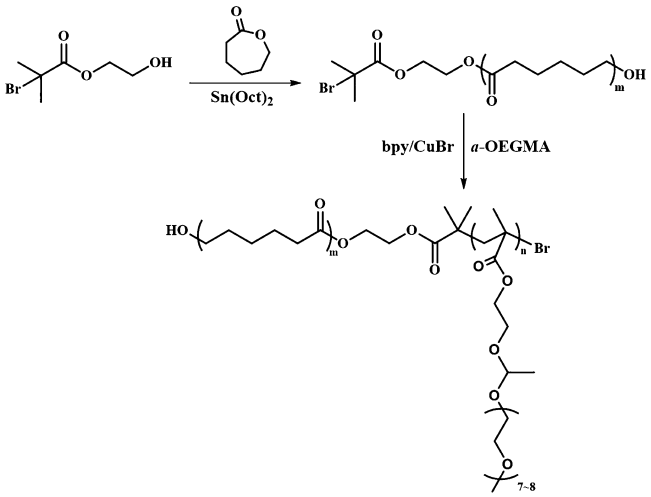


To evaluate the polymerization properties of *a*-OEGMA by ATRP, a series of polymers was synthesized by varying polymerization time. The molecular parameters of the resulting PCL-*b*-P(*a*-OEGMA)s were summarized in Table 1. Taking $PCL_{21}$-*b*-P(*a*-OEGMA)$_{11}$ (run 3 in Table 1) as an example, the DP of *a*-OEGMA was determined to be 11 by comparing the ratio of integrated intensity of peak f attributed to acetal methine to that of peak d assigned to PCL units (Figure 2a). All the three polymers show unimodal and symmetrical SEC elution peaks as well as a clear shift of the SEC elution traces toward higher molecular weight with increasing polymerization time (Figure 2b), which demonstrates well-controlled chain extension of *a*-OEGMA by ATRP. The precisely controlled polymerizations of *a*-OEGMA by CLRP technique are reflected by the pseudo-first-order kinetics (Figure 2c) and narrow PDI (<1.3; Table 1) during the polymerization process, which offers a robust route toward acidic pH-cleavable hydrophilic building block.

**Table 1. Summary of a Series of PCL-*b*-P(*a*-OEGMA) Polymers Prepared at Different Polymerization Time Using $PCL_{21}$ as a Macroinitiator**

| run | time[a] (h) | DP[b] | $M_n$[b] (kDa) | $M_n$[c] (kDa) | PDI[c] |
|---|---|---|---|---|---|
| 1 | 1.5 | 4 | 4.31 | 5.48 | 1.23 |
| 2 | 2.5 | 8 | 6.33 | 7.64 | 1.28 |
| 3 | 3.5 | 11 | 7.85 | 10.8 | 1.26 |
| 4 | 2.0 | 18 | 7.69 | 13.3 | 1.32 |

[a]Polymerization conditions, $[a\text{-OEGMA}]_0/[PCL]_0/[bpy]_0/[CuBr]_0$ = 20:1:2:1, $[OEGMA]_0$ = 0.5 mol/L in anisole for runs 1, 2, and 3. $[OEGMA]_0/[PCL]_0/[bpy]_0/[CuBr]_0$ = 30:1:2:1, $[OEGMA]_0$ = 0.5 mol/L in anisole for run 4 [b]Determined by $^{1}$H NMR analysis. [c]Determined by SEC-MALLS.

To demonstrate the advantages of *a*-OEGMA relative to the commercially available OEGMA for drug delivery applications, $PCL_{21}$-*b*-P(OEGMA)$_{18}$ diblock copolymer (Figures S6 and 3; run 4 in Table 1) with an almost identical MW for the hydrophilic block was also prepared as a pH-insensitive analogue using the commercially available OEGMA monomer ($M_n$ = 300 g/mol and 4−5 pendent EO units).

**Characterization of $PCL_{21}$-*b*-P(*a*-OEGMA)$_{11}$ Micelles.** The CMC of $PCL_{21}$-*b*-P(*a*-OEGMA)$_{11}$ was investigated using pyrene as a fluorescence probe. The fluorescence intensity keeps relatively constant at low concentrations, but increases dramatically at a certain concentration, indicating the formation of micelles. Such concentration was determined to be 9.33 mg/L for $PCL_{21}$-*b*-P(*a*-OEGMA)$_{11}$ (Figure S7) and 7.98 mg/L for $PCL_{21}$-*b*-P(OEGMA)$_{18}$ (Figure S8). The slightly lower CMC value of PCL-*b*-P(OEGMA)$_{18}$ relative to that of PCL-*b*-P(*a*-OEGMA)$_{11}$ implies the greater thermodynamic stability[38] of pH-insensitive micelles over pH-sensitive ones, which results likely from the different packing behaviors[38−40] caused by the hydrophilic POEGMA moiety with different DPs and brush-like structures, that is, P(*a*-OEGMA)$_{11}$ with long OEG brush and low DP versus P(OEGMA)$_{18}$ with short OEG brush and high DP, albeit their almost identical MW.

To evaluate the stability of self-assembled micelles, DLS was next used to determine the average hydrodynamic size of micelles self-assembled by $PCL_{21}$-*b*-P(a-OEGMA)$_{11}$ and $PCL_{21}$-*b*-P(OEGMA)$_{18}$ in both $ddH_2O$ and PBS (pH 7.4, 150 mM) at various polymer concentrations. The mean size recorded at different polymer concentrations ranges from approximately 110 to 150 nm (Figures S9 and S10). Such change is most likely relevant to the different aggregation numbers of polymer chains for micelle formation at various polymer concentrations above the CMC. Therefore, the largest size at 0.5 mg/mL of all the three concentrations probably results from the greatest aggregation number at this concentration. However, the statistical insignificance between each value implies the stability of both micelle formulations in salt medium and in diluted conditions.


DOI: 10.1021/acs.biomac.8b01001
Biomacromolecules 2018, 19, 3874−3882

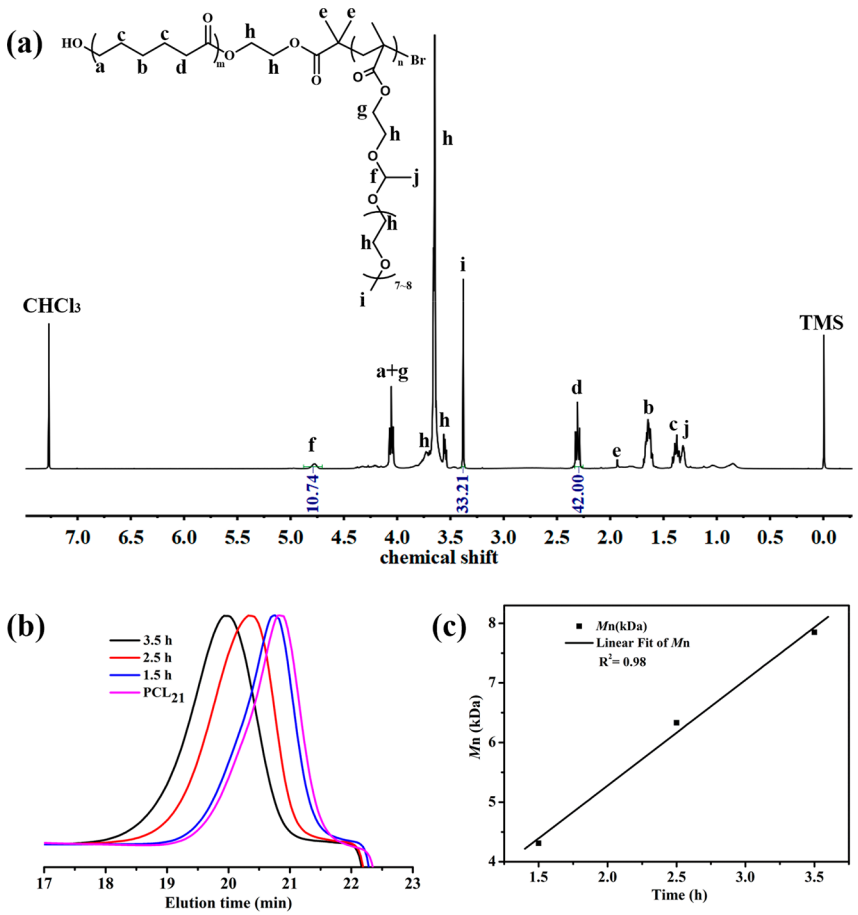


**Figure 2.** (a) $^1$H NMR spectrum of $PCL_{21}$-*b*-P(*a*-OEGMA)$_{11}$ in $CDCl_3$. (b) SEC elution traces of $PCL_{21}$-iBuBr and PCL-*b*-P(*a*-OEGMA) prepared at different polymerization time (eluent: DMF). (c) ATRP pseudo-first-order kinetics plot of PCL-*b*-P(*a*-OEGMA).

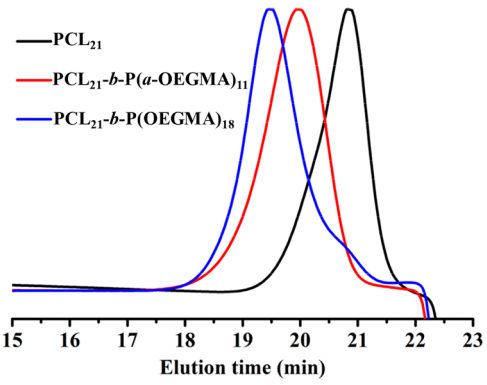


**Figure 3.** SEC elution traces of PCL, and $PCL_{21}$-*b*-P(*a*-OEGMA)$_{11}$ and $PCL_{21}$-*b*-P(OEGMA)$_{18}$ using DMF as an eluent.

The morphology of micelles self-assembled by $PCL_{21}$-*b*-P(*a*-OEGMA)$_{11}$ and $PCL_{21}$-*b*-P(OEGMA)$_{18}$ was visualized by TEM. Both polymers self-assembled into uniform nanoparticles with regularly spherical shape (Figures 4a and S11) and similar dimension in a dried state. The difference in the particle size between TEM and DLS measurements could be ascribed to the hydration effect, that is, the hydrophilic PEG segments are solvated in an aqueous phase and can be determined by DLS measurements but difficult to be observed under TEM observation.

**Acidic pH-Triggered Aggregation of $PCL_{21}$-*b*-P(*a*-OEGMA)$_{11}$ Micelles.** To verify the acidic pH-triggered cleavage of acetal links, the size change of $PCL_{21}$-*b*-P(*a*-OEGMA)$_{11}$ micelles incubated at different pH values of 7.4, 6.8, and 5.0 for various periods was monitored by DLS (Figure 5a).

The micelle size increased slightly from 118.5 to 143.9 nm after incubation at pH 7.4 for 48 h, however, such change is statistical insignificant, which implies the colloidal stability of the self-assembled micelles at the physiological pH.

In addition to the stability required at pH 7.4 for realizing long circulation, polymeric micelles must maintain certain structural integrity in the extracellular tumor microenvironment with a weakly acidic pH of 6.8 to facilitate efficiently cellular uptake. The micelles were thus incubated at pH 6.8 to evaluate the stability under this circumstance. The mean size kept almost stable around approximately 140 nm after incubation for 12 h and reached a plateau of 220 nm with further incubation of 24 and 72 h. Such an increase of micelle size is likely relevant to the minority cleavage of the acetal links, leading to a slight aggregation of the micelles.

However, incubation at pH 5.0 significantly promotes disassembly of micelles, which is reflected by the dramatically increased size and a broader size distribution. Notably, a bimodal distribution was clearly recorded for 48 h. The main population centered at approximately 504 nm probably implies that the majority of the self-assembled micelles have been subjected to acidic pH-triggered hydrolysis of acetal links and significant aggregation due to the deshielding of stabilizing corona composed of pendant OEG brushes. A few micelles


DOI: 10.1021/acs.biomac.8b01001
Biomacromolecules 2018, 19, 3874−3882

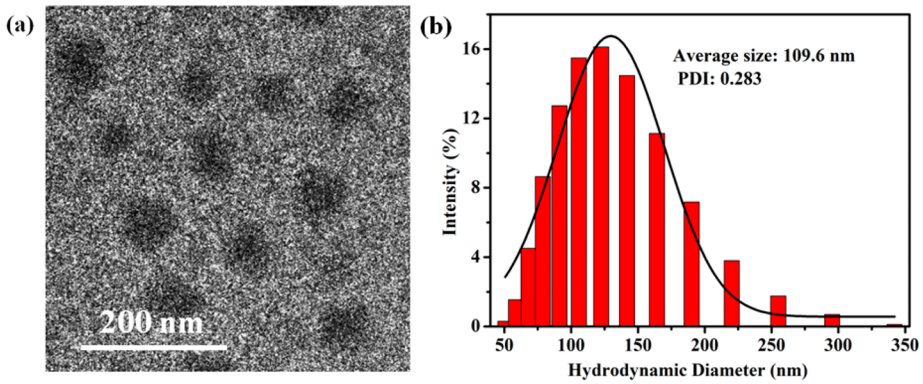


**Figure 4.** TEM image (a) and size distribution (b) of $PCL_{21}$-*b*-P(*a*-OEGMA)$_{11}$ micelles at a polymer concentration of 0.5 mg/mL.

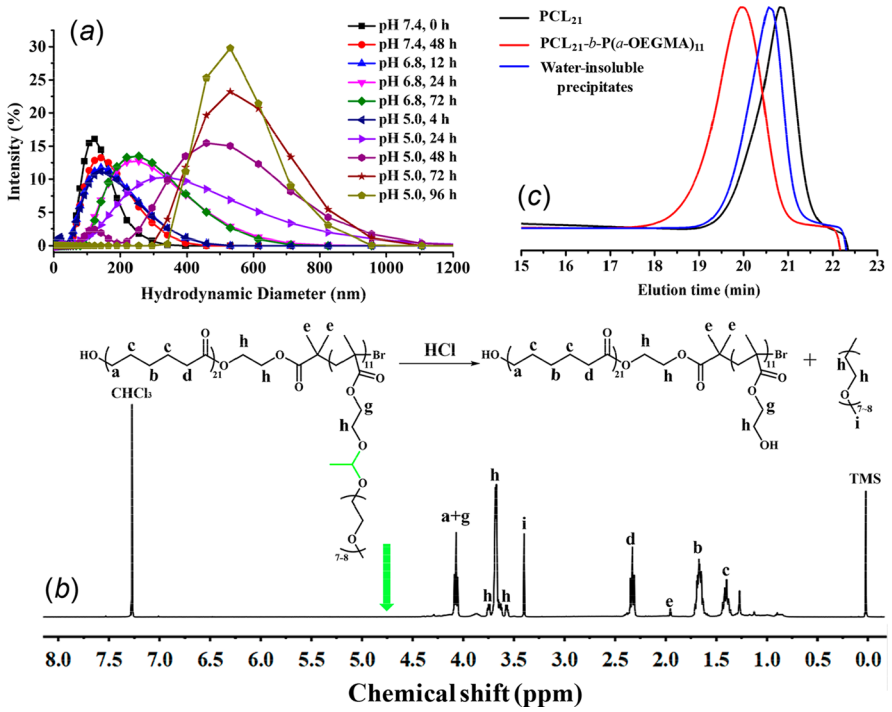


**Figure 5.** (a) DLS-monitored size change of $PCL_{21}$-*b*-P(*a*-OEGMA)$_{11}$ micelles after incubation at different pH values of 7.4, 6.8, and 5.0 for various periods at a polymer concentration of 0.25 mg/mL. (b) $^1$H NMR spectrum of the degraded products of $PCL_{21}$-*b*-P(*a*-OEGMA)$_{11}$ treated with hydrochloric acid in $CDCl_3$. (c) SEC elution traces of $PCL_{21}$-iBuBr, $PCL_{21}$-*b*-P(*a*-OEGMA)$_{11}$, and water-insoluble precipitates after degradation of $PCL_{21}$-*b*-P(*a*-OEGMA)$_{11}$ by hydrochloric acid.

remain intact, as evidenced by the presence of a small population centered at 122 nm, which is close to the mean size of the stable micelles (Figure 4b). The disappearance of this small population as well as similarly recorded mean sizes for prolonged incubation time of 72 and 96 h probably indicate the complete hydrolysis within 72 h.

To confirm the size variation monitored by DLS, TEM observation of $PCL_{21}$-*b*-P(*a*-OEGMA)$_{11}$ micelles after incubation at pH 6.8 and 5.0 for 24 h was performed (Figure S12a,b). Well-dispersed micelles with regularly spherical shape and uniform size were maintained even after incubation at pH 6.8 for 24 h (Figure S12a), demonstrating the stability of pH-sensitive micelles at the pH of the tumor microenvironment. The slightly increased size compared to that observed in water (Figure 4a) is most likely due to the minority cleavage of the acetal links in the micelle structure, which exerts a negligible effect on the stability of the self-assembled micelles. However, incubation at pH 5.0 for 24 h led to the formation of densely arranged micelle aggregates with irregularly spherical shape and nonuniform dimension (Figure S12b). More importantly, the formation of aggregates is strongly evidenced by a significantly increased mean size and broader size distribution at pH 5.0 relative to those observed in water and pH 6.8, as well as the clearly visualized coalescences of individual small micelles. Taken together, the TEM results are in good agreement with the DLS data, confirming the stability of pH-sensitive micelles at pH 6.8 and occurrence of aggregation at pH 5.0.

$^1$H NMR analysis was also utilized to verify the acidic pH-triggered hydrolysis of acetal links. A total of 10 mg of $PCL_{21}$-*b*-P (*a*-OEGMA)$_{11}$ was first dissolved in 4.5 mL of $H_2O$ followed by addition of hydrochloric acid aqueous solution (36 wt %, 1 mL) and stirred at 25 °C for 24 h. Note that the transparent polymer solution became cloudy gradually, likely due to the detachment of stabilizing pendant OEG brushes and significantly reduced solubility of the degraded products. The



DOI: 10.1021/acs.biomac.8b01001
Biomacromolecules 2018, 19, 3874−3882

mixture was finally freeze-dried and subjected to $^1$H NMR analysis (Figure 5b), which reveals presence of characteristic signals of PEG and PCL moieties, but complete loss of characteristic peaks of acetal links at $\delta$ 4.79−4.84 ppm (highlighted using green color and arrow in the structural formula and in the $^1$H NMR spectrum, respectively). The results support acid-cleavage of acetal links in $PCL_{21}$-*b*-P(*a*-OEGMA)$_{11}$.

In addition, SEC-MALLS analyses were used to determine the MW of the degraded products. The water-insoluble precipitates were collected by filtration and subjected to vacuum-drying prior to SEC-MALLS measurements. As expected, the degraded products without pendant OEG brushes show significantly decreased MW relative to the parent $PCL_{21}$-*b*-P(*a*-OEGMA)$_{11}$, and slightly increased MW compared to $PCL_{21}$-iBuBr (Figure 5c), which confirms the scission of acetal links rather than the hydroplysis of polyester under acidic condition.

To further provide an insight into the acidic-pH triggered degradation of $PCL_{21}$-*b*-P(*a*-OEGMA)$_{11}$, the fully degraded product, $PCL_{21}$-*b*-P(2-hydroxyethyl methacrylate)$_{11}$ ($PCL_{21}$-*b*-P(HEMA)$_{11}$), was also synthesized by ATRP of HEMA using $PCL_{21}$-iBuBr macroinitiator given that the full degradation of the hydrophilic P(*a*-OEGMA) block generates the P(HEMA) moiety with somewhat hydrophilicity. The successful synthesis of $PCL_{21}$-*b*-P(HEMA)$_{11}$ with desired polymer composition was confirmed by $^1$H NMR (Figure S13) and SEC-MALLS (Figure S14) analyses. The average size of the self-assemblies formed by $PCL_{21}$-*b*-P(HEMA)$_{11}$ was determined by DLS to be 422.6 and 467.7 nm in water and PBS (pH 7.4), respectively (Figure S15), which probably indicates the formation of large micelle aggregates due to the significantly decreased hydrophilicity of P(HEMA) block relative to P(*a*-OEGMA) segment. TEM observation of $PCL_{21}$-*b*-P(HEMA)$_{11}$ reveals dense arrangement of nanoparticles with irregularly spherical shape and nonuniform size (Figure S12c), further confirming self-assembly of $PCL_{21}$-*b*-P(HEMA)$_{11}$ into unstable aggregates. The results agree well with the acidic pH-triggered aggregation of $PCL_{21}$-*b*-P(*a*-OEGMA)$_{11}$ micelles revealed by DLS (Figure 5a) and TEM (Figure S12b) measurements.

**In Vitro Drug Loading and Drug Release Study.** Doxorubicin (Dox) was chosen as a modal drug and encapsulated in $PCL_{21}$-*b*-P(*a*-OEGMA)$_{11}$ and $PCL_{21}$-*b*-P(OEGMA)$_{18}$ micelles by dialysis method. The slightly lower CMC value and greater stability of PCL-*b*-P(OEGMA)$_{18}$ micelles relative to PCL-*b*-P(*a*-OEGMA)$_{11}$ formulations contribute to the smaller size and greater drug-loading capacity of PCL-*b*-P(OEGMA)$_{18}$ micelles (Table 2).

To validate the acidic pH-triggered drug release, in vitro drug release profiles were investigated in buffer solutions with three different pHs of 7.4, 6.8, and 5.0, respectively (Figure 6). The Dox-loaded $PCL_{21}$-*b*-P(*a*-OEGMA)$_{11}$ micelles showed almost identical drug release behaviors at pH 7.4 and 6.8, demonstrating their apparent stability at the physiological pH and the pH of tumor microenvironment. Shift of release medium from pH 7.4 or 6.8 to 5.0 promoted Dox release from $PCL_{21}$-*b*-P(OEGMA)$_{18}$ micelles due to the increased solubility of protonated Dox under the acidic conditions.[41,42] More importantly, nearly 90% of Dox was released at pH 5.0 for Dox-loaded $PCL_{21}$-*b*-P(*a*-OEGMA)$_{11}$ micelles in 72 h, whereas approximately 50% Dox release was recorded at pH 5.0 for Dox-loaded $PCL_{21}$-*b*-P(OEGMA)$_{18}$ micelles in the same period. The significantly increased cumulative drug release is attributed to the acidic pH-triggered cleavage of acetal links for efficient destabilization of $PCL_{21}$-*b*-P(*a*-OEGMA)$_{11}$ micelles and formation of micelle aggregates toward promoted drug release.

**Table 2. Summarized Properties of Blank and Drug-Loaded $PCL_{21}$-*b*-P(*a*-OEGMA)$_{11}$ and $PCL_{21}$-*b*-P(OEGMA)$_{18}$ Micelles**

| micelle constructs | size (nm) | PDI | CMC (mg/L) | DLC (%) | EE (%) |
|---|---|---|---|---|---|
| $PCL_{21}$-*b*-P(*a*-OEGMA)$_{11}$ | 109.6 | 0.283 | 9.33 | | |
| $PCL_{21}$-*b*-P(OEGMA)$_{18}$ | 105.3 | 0.216 | 7.98 | | |
| Dox-loaded $PCL_{21}$-*b*-P(*a*-OEGMA)$_{11}$ | 147.6 | 0.250 | | 5.76 | 5.88 |
| Dox-loaded $PCL_{21}$-*b*-P(OEGMA)$_{18}$ | 124.7 | 0.271 | | 6.16 | 6.78 |

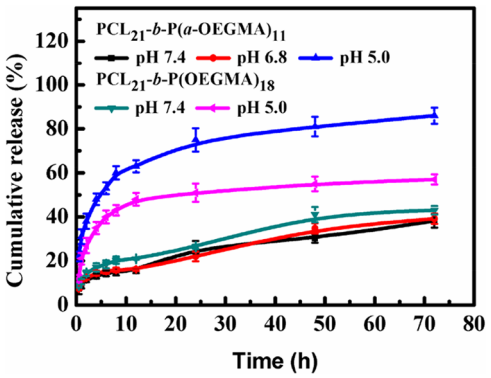


**Figure 6.** In vitro drug release profiles of Dox-loaded $PCL_{21}$-*b*-P(*a*-OEGMA)$_{11}$ and $PCL_{21}$-*b*-P(OEGMA)$_{18}$ micelles at different conditions.

**In Vitro Cellular Uptake and Cytotoxicity Studies.** The cellular uptake efficiency was first evaluated using confocal microscopy. Dox fluorescence was clearly observed in the cytoplasm and/or nuclei of cells incubated with free Dox or both Dox-loaded micelles for 4 h (Figure 7), indicating that both micelle constructs can efficiently transport the anticancer drug to the cells and subsequently undergo intracellular trafficking. Then the cellular uptake was further quantified

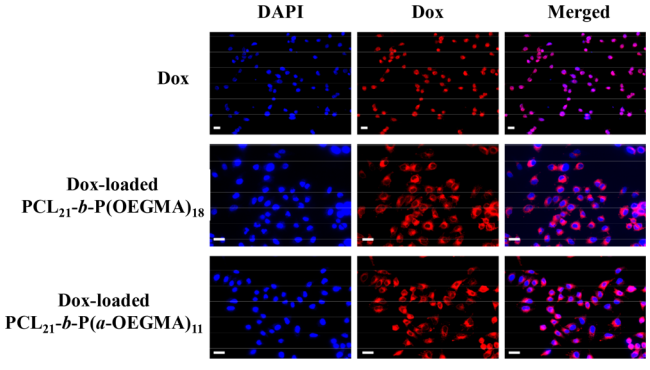


**Figure 7.** Confocal imaging of free DOX (red), Dox-loaded $PCL_{21}$-*b*-P(OEGMA)$_{18}$ and $PCL_{21}$-*b*-P(*a*-OEGMA)$_{11}$ micelles uptake in A549 cells (nuclei stained blue with DAPI). Cells were treated with free DOX or polymer constructs at 25% of its IC50 value to minimize cell death. The scale bar represents 50 $\mu$m.



DOI: 10.1021/acs.biomac.8b01001
Biomacromolecules 2018, 19, 3874−3882

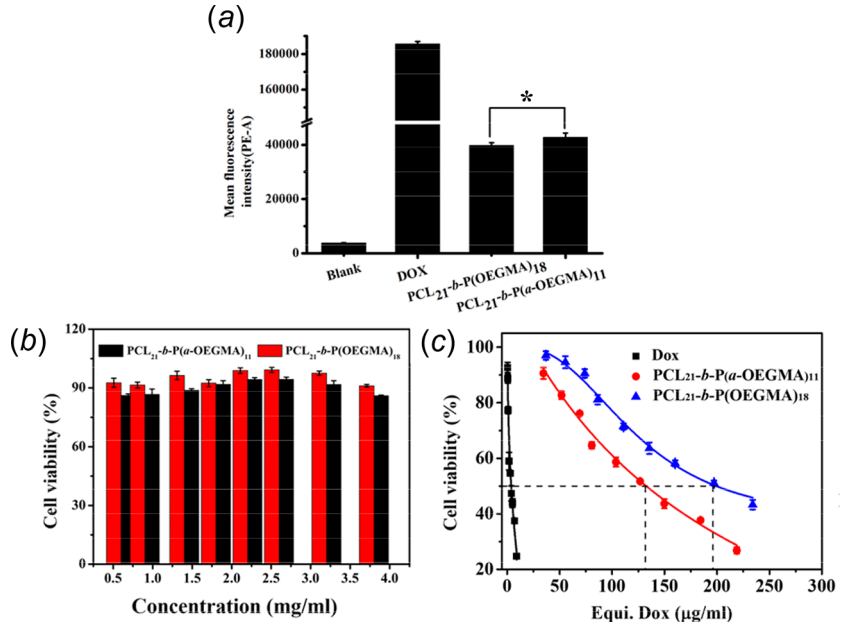


**Figure 8.** (a) Quantitive measurements of the mean fluorescence intensity after incubation with free Dox, Dox-loaded micelles of $PCL_{21}$-*b*-P(*a*-OEGMA)$_{11}$ and $PCL_{21}$-*b*-P(OEGMA)$_{18}$ in A549 cells via flow cytometry (4 h incubation, Dox concentration = 20 μg/mL, and 10000 cells were counted). The data were expressed as mean ± SD, $n = 3$ (*$p < 0.01$). Viability of A549 cells exposed to (b) blank micelles of $PCL_{21}$-*b*-P(OEGMA)$_{18}$, $PCL_{21}$-*b*-P(*a*-OEGMA)$_{11}$ and (c) free Dox, Dox-loaded micelles of $PCL_{21}$-*b*-P(*a*-OEGMA)$_{11}$ and $PCL_{21}$-*b*-P(OEGMA)$_{18}$.

using flow cytometry (FCM) analyses (Figure 8a). The mean fluorescence intensity of A549 cells treated with both Dox-loaded micelles was clearly observed in 4 h. The cells treated with free Dox presented much higher fluorescence intensity than the cells incubated with micelle formulations most likely due to the faster diffusion rate of Dox in cells with a mechanism of direct membrane permeation. Interestingly, the Dox-loaded $PCL_{21}$-*b*-P(*a*-OEGMA)$_{11}$ micelles mediated slightly higher fluorescence intensity with statistical significance relative to the pH-insensitive analogues, which probably implies the stronger ability for the pH-sensitive micelles to deliver the anticancer drug into the cancer cells.

Finally, the cytotoxicity of Dox-loaded $PCL_{21}$-*b*-P(*a*-OEGMA)$_{11}$ and $PCL_{21}$-*b*-P(OEGMA)$_{18}$ micelles to A549 cells was assessed by 3-(4,5-dimethylthiazol-2-yl)-5-(3-carboxymethoxyphenyl)-2-(4-sulfophenyl)-2*H*-tetrazolium (MTS) cell viability assay. Both blank micelles were nontoxic to A549 cells up to a concentration of 3.8 mg/mL (Figure. 8b). The half maximal inhibitory concentration (IC50) of free Dox, Dox-loaded $PCL_{21}$-*b*-P(*a*-OEGMA)$_{11}$ and $PCL_{21}$-*b*-P(OEGMA)$_{18}$ micelles is 3.64 (3.13, 4.24), 128.5 (122.2, 135.1), and 194.7 (180.3, 210.3) μg/mL, respectively (Figure 8c). The increased $IC_{50}$ of Dox-loaded micelles relative to free Dox is likely attributed to the slower internalization mechanism and the release kinetics of free drug from the micelles. Most importantly, the Dox-loaded $PCL_{21}$-*b*-P(*a*-OEGMA)$_{11}$ micelles showed significantly greater therapeutic efficacy, that is, lower $IC_{50}$ value than the pH-insensitive counterparts due to the efficient destabilization and aggregation of micelles and subsequently promoted drug release in the intracellular acidic pH environment.

## CONCLUSIONS

In summary, to develop a facile and universal alternative toward tumor acidic pH-responsive polymers, we reported in this study successful synthesis of a dual functional monomer, *a*-OEGMA that integrates the merits of commercially available OEGMA monomer for both extracellular stabilization of particulates and CLRP-mediated polymerization properties, and an acidic pH-cleavage acetal link for efficient intracellular destabilization of polymeric carriers. Amphiphilic block copolymers, $PCL_{21}$-*b*-P(*a*-OEGMA)$_{11}$ with pendant acidic pH-cleavable OEG brushes were further prepared using this monomer. The delivery efficacy evaluated by an in vitro drug release study and flow cytometry analyses, as well as an in vitro cytotoxicity study further confirmed promoted drug release at pH 5.0, greater cellular uptake and cytotoxicity of Dox-loaded pH-sensitive micelles of $PCL_{21}$-*b*-P(*a*-OEGMA)$_{11}$ relative to the pH-insensitive analogues of $PCL_{21}$-*b*-P(OEGMA)$_{18}$. The *a*-OEGMA monomer developed herein therefore presents a facile and robust means toward tumor acidic pH-responsive polymers as well as provides one solution to the trade-off between extracellular stability and intracellular high therapeutic efficacy of drug delivery systems.

## ASSOCIATED CONTENT

### Supporting Information

The Supporting Information is available free of charge on the ACS Publications website at DOI: 10.1021/acs.biomac.8b01001.

Experimental details, $^1$H NMR of VEMA, $^{13}$C NMR, FT-IR, HRMS data of *a*-OEGMA, $^1$H NMR specta of PCL-iBuBr and $PCL_{21}$-*b*-P(OEGMA)$_{18}$, CMC determinations of $PCL_{21}$-*b*-P(*a*-OEGMA)$_{11}$ and $PCL_{21}$-*b*-P(OEGMA)$_{18}$, TEM images and size distributions of $PCL_{21}$-*b*-P(OEGMA)$_{18}$ micelles, average size of $PCL_{21}$-*b*-P(*a*-OEGMA)$_{11}$ and $PCL_{21}$-*b*-P(OEGMA)$_{18}$ micelles at various polymer concentrations in water and PBS (pH 7.4, 150 mM), TEM images of $PCL_{21}$-*b*-P(*a*-OEGMA)$_{11}$ micelles after incubation at pH 6.8 and 5.0 for 24 h, and micelle aggregates formed by $PCL_{21}$-*b*-P(HEMA)$_{11}$, $^1$H NMR spectrum and SEC elution trace of $PCL_{21}$-*b*-


DOI: 10.1021/acs.biomac.8b01001
Biomacromolecules 2018, 19, 3874−3882

$P(HEMA)_{11}$, size distributions of $PCL_{21}$-*b*-$P(HEMA)_{11}$ in water and PBS (pH 7.4, 150 mM), standard curve of Dox in PBS (pH 7.4) are available in Figures S1−S16 (PDF).

## AUTHOR INFORMATION


### Corresponding Authors

*E-mail: weih@lzu.edu.cn.
*E-mail: 1126@hbtcm.edu.cn.

### ORCID

Hua Wei: 0000-0002-5139-9387

### Author Contributions

‡These authors contributed equally to this paper.


### Notes

The authors declare no competing financial interest.

## ACKNOWLEDGMENTS

The authors acknowledge the financial support from the National Natural Science Foundation of China (51473072 and 21504035), the Thousand Young Talent Program, the Open Research Fund of State Key Laboratory of Polymer Physics and Chemistry, Changchun Institute of Applied Chemistry, Chinese Academy of Sciences, and the Young Crop Plan of Hubei University of Traditional Chinese Medicine (2017ZZX021).

## REFERENCES


(1) Cayre, O. J.; Chagneux, N.; Biggs, S. Stimulus-Responsive Core-Shell Nanoparticles: Synthesis and Applications of Polymer Based Aqueous Systems. *Soft Matter* **2011**, *7*, 2211−2234.

(2) Felber, A. E.; Dufresne, M. H.; Leroux, J. C. pH-Sensitive Vesicles, Polymeric Micelles, and Nanospheres Prepared with Polycarboxylates. *Adv. Drug Delivery Rev.* **2012**, *64*, 979−992.

(3) Fleige, E.; Quadir, M. A.; Haag, R. Stimuli-Responsive Polymeric Nanocarriers for the Controlled Transport of Active Compounds: Concepts and Applications. *Adv. Drug Delivery Rev.* **2012**, *64*, 866−884.

(4) Tian, H.; Tang, Z.; Zhuang, X.; Chen, X.; Jing, X. Biodegradable Synthetic Polymers: Preparation, Functionalization and Biomedical Application. *Prog. Polym. Sci.* **2012**, *37*, 237−280.

(5) Zhang, Q.; Ko, N. R.; Oh, J. K. Recent Advances in Stimuli-Responsive Degradable Block Copolymer Micelles: Synthesis and Controlled Drug Delivery Applications. *Chem. Commun.* **2012**, *48*, 7542−7552.

(6) Wei, H.; Zhuo, R. X.; Zhang, X. Z. Design and Development of Polymeric Micelles with Cleavable Links for Intracellular Drug Delivery. *Prog. Polym. Sci.* **2013**, *38*, 503−535.

(7) Binauld, S.; Scarano, W.; Stenzel, M. H. pH-Triggered Release of Platinum Drugs Conjugated to Micelles via an Acid-Cleavable Linker. *Macromolecules* **2012**, *45*, 6989−6999.

(8) Jackson, A. W.; Fulton, D. A. Making Polymeric Nanoparticles Stimuli-Responsive with Dynamic Covalent Bonds. *Polym. Chem.* **2013**, *4*, 31−45.

(9) Huynh, V. T.; Binauld, S.; Souza, P. L.; Stenzel, M. H. Acid Degradable Cross-Linked Micelles for the Delivery of Cisplatin: A Comparison with Nondegradable Cross-Linker. *Chem. Mater.* **2012**, *24*, 3197−3211.

(10) Liu, X.; Tian, Z.; Chen, C.; Allcock, H. R. UV-Cleavable Unimolecular Micelles: Synthesis and Characterization toward Photocontrolled Drug Release Carriers. *Polym. Chem.* **2013**, *4*, 1115−1125.

(11) Nishiyama, N.; Iriyama, A.; Jang, W. D.; Miyata, K.; Itaka, K.; Inoue, Y.; Takahashi, H.; Yanagi, Y.; Tamaki, Y.; Koyama, H.; Kataoka, K. Light-Induced Gene Transfer from Packaged DNA Enveloped in a Dendrimeric Photosensitizer. *Nat. Mater.* **2005**, *4*, 934−941.

(12) Founi, M. E.; Soliman, S. M. A.; Vanderesse, R.; Acherar, S.; Guedon, E.; Chevalot, I.; Babin, J.; Six, J. L. Light-Sensitive Dextran-Covered PNBA Nanoparticles as Triggered Drug Delivery Systems: Formulation, Characteristics and Cytotoxicity. *J. Colloid Interface Sci.* **2018**, *514*, 289−298.

(13) Sun, C.; Ji, S.; Li, F.; Xu, H. Diselenide-Containing Hyperbranched Polymer with Light-Induced Cytotoxicity. *ACS Appl. Mater. Interfaces* **2017**, *9*, 12924−12929.

(14) Kim, H.; Man, H. B.; Saha, B.; Kopacz, A. M.; Lee, O. S.; Schatz, G. C.; Ho, D.; Liu, W. K. Multiscale Simulation as a Framework for the Enhanced Design of Nanodiamond-Polyethylenimine-Based Gene Delivery. *J. Phys. Chem. Lett.* **2012**, *3*, 3791−3797.

(15) Vaijayanthimala, V.; Lee, D. K.; Kim, S. V.; Yen, A.; Tsai, N.; Ho, D.; Chang, H. C.; Shenderova, O. Nanodiamond-Mediated Drug Delivery and Imaging: Challenges and Opportunities. *Expert Opin. Drug Delivery* **2015**, *12*, 735−749.

(16) Lai, H.; Chen, F.; Lu, M.; Stenzel, M. H.; Xiao, P. Polypeptide-Grafted Nanodiamonds for Controlled Release of Melittin to Treat Breast Cancer. *ACS Macro Lett.* **2017**, *6*, 796−801.

(17) Zhao, J.; Lu, M.; Lai, H.; Lu, H.; Lalevée, J.; Barner-Kowollik, C.; Stenzel, M. H.; Xiao, P. Delivery of Amonafide from Fructose-Coated Nanodiamonds by Oxime Ligation for the Treatment of Human Breast Cancer. *Biomacromolecules* **2018**, *19*, 481−489.

(18) Deng, C.; Jiang, Y.; Cheng, R.; Meng, F.; Zhong, Z. Biodegradable Polymeric Micelles for Targeted and Controlled Anticancer Drug Delivery: Promises, Progress and Prospects. *Nano Today* **2012**, *7*, 467−480.

(19) Ganta, S.; Devalapally, H.; Shahiwala, A.; Amiji, M. A Review of Stimuli-Responsive Nanocarriers for Drug and Gene Delivery. *J. Controlled Release* **2008**, *126*, 187−204.

(20) Lee, E. S.; Gao, Z.; Bae, Y. H. Recent Progress in Tumor pH Targeting Nanotechnology. *J. Controlled Release* **2008**, *132*, 164−170.

(21) Gillies, E. R.; Goodwin, A. P.; Fréchet, J. M. J. Acetals as pH-Sensitive Linkages for Drug Delivery. *Bioconjugate Chem.* **2004**, *15*, 1254−1263.

(22) Jain, R.; Standley, S. M.; Fréchet, J. M. J. Synthesis and Degradation of pH-Sensitive Linear Poly(amidoamine)s. *Macromolecules* **2007**, *40*, 452−457.

(23) Tonhauser, C.; Schüll, C.; Dingels, C.; Frey, H. Branched Acid-Degradable, Biocompatible Polyether Copolymers via Anionic Ring-Opening Polymerization Using an Epoxide Inimer. *ACS Macro Lett.* **2012**, *1*, 1094−1097.

(24) Bae, Y.; Fukushima, S.; Harada, A.; Kataoka, K. Design of Environment-Sensitive Supramolecular Assemblies for Intracellular Drug Delivery: Polymeric Micelles that are Responsive to Intracellular pH Change. *Angew. Chem., Int. Ed.* **2003**, *42*, 4640−4643.

(25) Zhu, L.; Tu, C.; Zhu, B.; Su, Y.; Pang, Y.; Yan, D.; Wu, J.; Zhu, X. Construction and Application of pH-Triggered Cleavable Hyperbranched Polyacylhydrazone for Drug Delivery. *Polym. Chem.* **2011**, *2*, 1761−1768.

(26) Du, J. Z.; Du, X. J.; Mao, C. Q.; Wang, J. Tailor-Made Dual pH-Sensitive Polymer-Doxorubicin Nanoparticles for Efficient Anticancer Drug Delivery. *J. Am. Chem. Soc.* **2011**, *133*, 17560−17563.

(27) Cheng, J.; Ji, R.; Gao, S. J.; Du, F. S.; Li, Z. C. Facile Synthesis of Acid-Labile Polymers with Pendent Ortho Esters. *Biomacromolecules* **2012**, *13*, 173−179.

(28) Heller, J.; Barr, J.; Ng, S. Y.; Abdellauoi, K. S.; Gurny, R. Poly(ortho esters): Synthesis, Characterization, Properties and Uses. *Adv. Drug Delivery Rev.* **2002**, *54*, 1015−1039.

(29) Liu, T.; Li, X.; Qian, Y.; Hu, X.; Liu, S. Multifunctional pH-Disintegrable Micellar Nanoparticles of Asymmetrically Functionalized β-Cyclodextrin-Based Star Copolymer Covalently Conjugated with Doxorubicin and DOTA-Gd Moieties. *Biomaterials* **2012**, *33*, 2521−2531.

(30) Wang, H.; He, J.; Zhang, M.; Tao, Y.; Li, F.; Tam, K. C.; Ni, P. Biocompatible and Acid-Cleavable Poly(ε-Caprolactone)-Acetal-Poly(Ethylene Glycol)-Acetal-Poly(ε-Caprolactone) Triblock Copoly-




DOI: 10.1021/acs.biomac.8b01001
*Biomacromolecules* 2018, 19, 3874−3882

mers: Synthesis, Characterization and pH-Triggered Doxorubicin Delivery. *J. Mater. Chem. B* **2013**, *1*, 6596−6607.
(31) Miao, K.; Shao, W.; Liu, H.; Zhao, Y. Synthesis and Properties of a Dually Cleavable Graft Copolymer Comprising Pendant Acetal Linkages. *Polym. Chem.* **2014**, *5*, 1191−1201.
(32) Wei, H.; Pahang, J. A.; Pun, S. H. Optimization of Brush-Like Cationic Copolymers for Nonviral Gene Delivery. *Biomacromolecules* **2013**, *14*, 275−284.
(33) Zhang, H.; Ruckenstein, E. Graft Copolymers by Combined Anionic and Cationic Polymerizations Based on the Homopolymerization of a Bifunctional Monomer. *Macromolecules* **1998**, *31*, 746−752.
(34) Rikkou-Kalourkoti, M.; Matyjaszewski, K.; Patrickios, C. S. Synthesis, Characterization and Thermolysis of Hyperbranched Homo- and Amphiphilic Co-Polymers Prepared Using an Inimer Bearing a Thermolyzable Acylal Group. *Macromolecules* **2012**, *45*, 1313−1320.
(35) Aoshima, S.; Sugihara, S.; Shibayama, M.; Kanaoka, S. Synthesis and Self-Association of Stimuli-Responsive Diblock Copolymers by Living Cationic Polymerization. *Macromol. Symp.* **2004**, *215*, 151−164.
(36) Schild, H. G. Poly(*N*-isopropylacrylamide): Experiment, Theory and Application. *Prog. Polym. Sci.* **1992**, *17*, 163−249.
(37) Hoffman, A. S. " Intelligent" Polymers in Medicine and Biotechnology. *Macromol. Symp.* **1995**, *98*, 645−664.
(38) Wang, Y.; Wu, Z.; Ma, Z.; Tu, X.; Zhao, S.; Wang, B.; Ma, L.; Wei, H. Promotion of Micelle Stability via a Cyclic Hydrophilic Moiety. *Polym. Chem.* **2018**, *9*, 2569−2573.
(39) Chu, Y.; Zhang, W.; Lu, X.; Mu, G.; Zhang, B.; Li, Y.; Cheng, S. Z. D.; Liu, T. Rational Controlled Morphological Transitions in the Self-Assembled Multi-Headed Giant Surfactants in Solution. *Chem. Commun.* **2016**, *52*, 8687−8690.
(40) Zhang, W.; Huang, M.; Su, H.; Zhang, S.; Yue, K.; Dong, X. H.; Li, X.; Liu, H.; Zhang, S.; Wesdemiotis, C.; Lotz, B.; Zhang, W. B.; Li, Y.; Cheng, S. Z. D. Toward Controlled Hierarchical Heterogeneities in Giant Molecules with Precisely Arranged Nano Building Blocks. *ACS Cent. Sci.* **2016**, *2*, 48−54.
(41) Prabaharan, M.; Grailer, J. J.; Pilla, S.; Steeber, D. A.; Gong, S. Folate-Conjugated Amphiphilic Hyperbranched Block Copolymers Based on Boltorn H40, Poly(L-lactide) and Poly(ethylene glycol) for Tumor-Targeted Drug Delivery. *Biomaterials* **2009**, *30*, 3009−3019.
(42) Wang, M.; Zhang, X.; Peng, H.; Zhang, M.; Zhang, X.; Liu, Z.; Ma, L.; Wei, H. Optimization of Amphiphilic Miktoarm Star Copolymers for Anticancer Drug Delivery. *ACS Biomater. Sci. Eng.* **2018**, *4*, 2903−2910.



DOI: 10.1021/acs.biomac.8b01001
*Biomacromolecules* 2018, 19, 3874−3882